10/11/17/88 JS ①

DR# 0600-9

UCID--21532

DE89 002540

Summary of Mirror Experiments Relevant to Beam-Plasma Neutron Source

A.W. Molvik

October 18, 1988

Lawrence
Livermore
National
Laboratory

Work performed under the auspices of the U.S. Department of Energy by the Lawrence Livermore National Laboratory under Contract W-7405-Eng-48.

MASTER

DISCLAIMER

Printed in the United States of America
Available from
National Technical Information Service
U.S. Department of Commerce
5285 Port Royal Road
Springfield, VA 22161

Price Code	Page Range
A01	Microfiche
Papercopy Prices	
A02	001-050
A03	051-100
A04	101-200
A05	201-300
A06	301-400
A07	401-500
A08	501-600
A09	601

November 2, 1988

Summary of Mirror Experiments Relevant to Beam-Plasma Neutron Source

A.W. Molvik
Lawrence Livermore National Laboratory,
University of California,
Livermore, California 94550

1. Introduction

A promising design for a deuterium-tritium (DT) neutron source is based on the injection of neutral beams into a dense, warm plasma column. Its purpose is to test materials for possible use in fusion reactors. A series of designs have evolved, from a 4-T version [1] to an 8-T version [2]. Intense fluxes of 5-10 MW/m^2 is achieved at the plasma surface, sufficient to complete end-of-life tests in one to two years. An intense neutron flux of 5 to 10 MW/m^2 is achieved at the plasma surface, sufficient to complete end-of-life tests in one to two years. In this report, we review data from earlier mirror experiments that are relevant to such neutron sources. Most of these data are from 2XIIB, which was the only facility to ever inject 5 MW of neutral beams into a single mirror call.

The major physics issues for a beam-plasma neutron source are magnetohydrodynamic (MHD) equilibrium and stability, microstability, startup, cold-ion fueling of the midplane to allow two-component reactions, and operation in the Spitzer conduction regime, where the power is removed to the ends by an axial gradient in the electron temperature T_e. We show

Table 1: Summary of 2XIIB field-reversal experiments from Ref. 1.

Date	B_{vac} (kG)	I_{beam} (A)	R_p (cm)	m (MA · cm^2)	E_i (keV)	T (eV)	$\Delta B/B$
March 30, 1977	6.7	400	8.7	18	12.5	75	0.4
April 14, 1977	4.35	400	6.5	14	10.2	50	0.9
September 12, 1977	6.7	500	6.5	14	12.4	140	0.6

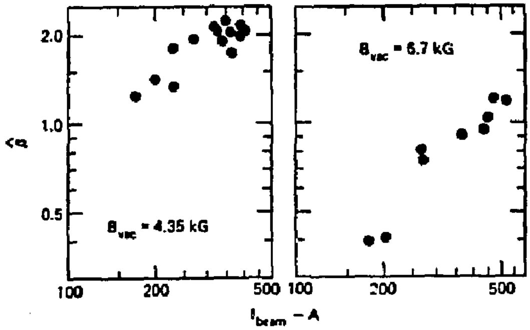

Figure 1: Peak plasma beta vs injected beam current. These data show 2XIIB-confined stable plasma with beta > 1.0.

in this report that the conditions required for a neutron source have now been demonstrated in experiments.

2. MHD Equilibrium and Stability

The 2XIIB facility confined plasma in a minimum-B geometry with peak beta as high as 2 locally, resulting in a reduction of the magnetic field on-axis to 0.10 of the vacuum value, as listed in Table 1 [Ref. 3]. As shown in Fig. 1, the value of beta increased linearly with the neutral-beam current, indicating that beta was not limited by equilibrium or stability.

The value of beta could be limited theoretically by lack of equilibrium, where the plasma pressure gradient relative to the axial magnetic field gradient is sufficiently large that the magnetic field cannot maintain its shape and confine the plasma. This is known as the mirror

Table 2: Summary of experimental measurement[2] for plasma of varing $R_\mathrm{p}/a_\mathrm{a}$ for constant $\hat{\beta} = 0.40 \pm 0.05$.

Case	R_p (cm)	L_p (cm)	E_i (keV)	a_i (cm)	$R_\mathrm{p}/a_\mathrm{i}$	$\hat{n}$ 10^{13} (cm^{-3})	$\hat{T}_e$ (eV)	$\hat{n}\tau_\mathrm{E}$	$\hat{n}\tau_\mathrm{D}$	$\hat{n}\tau_\mathrm{p}$
								10^{10}($\mathrm{cm}^{-3}\cdot$s)		
1	5.5	16	12.4	3.4	1.6	4.0	60 ± 10	4.2 ± 0.5	5.8	5.9 ± 0.3
2	13.5	20	13.0	3.5	3.9	3.5	83 ± 15	4.5 ± 0.5	9.4	5.5 ± 0.5
3	14.0	20	12.3	2.9	4.8	5.0	128 ± 30	5.6 ± 0.9	18.0	6.5 ± 0.5
4	14.0	20	12.0	2.3	6.0	3.6	111 ± 15	5.7 ± 0.9	7.3	5.4 ± 0.4

mode, and its beta limit is increased by a higher mirror ratio. Flute interchange stability can also limit the beta. Increasing the radial well depth (i.e., good curvature of magnetic field lines) increases the beta limit for flute interchange. Apparently, both the mirror ratio and the radial well depth were sufficiently large in 2XIIB.

In extrapolating results from 2XIIB to other devices, it is necessary to keep in mind the geometry that may have influenced stability. First, the 2XIIB plasma was short, 2.5 to 5 gyroradii long, where a gyroradius a_i ranges from 3.5 to 7 cm, depending on beta. Second, the plasma radius was small, with $r_\mathrm{p}/a_\mathrm{i} \approx$ 1 to 2. These factors invalidate the long-thin approximation in which beta cannot exceed unity without reversing the magnetic field. It is also apparent that Finite Larmor radius (FLR) effects could be very strong. However, in other experiments [4] plasmas of radius as large as $r_\mathrm{p}/a_\mathrm{i} = 6$ (twice that planned in a beam-plasma neutron source) were confined at betas of 0.4 with no evidence of a beta limit (see Table 2). The plasma beta was limited by the available neutral beam power in this as in the other cases.

The neutron source requires betas of 0.6 [Ref. 1] for the 4 T version, or 0.2 [Ref. 2] in the 8 T version. The 2XIIB results showed stability to a much higher beta value of 2.0 with small-radius plasmas, and to nearly as high a beta in a larger-radius plasma as that planned for a neutron source. MHD stability appears assured for either version if we use a minimum-B coil at the hot-ion plasma. A more attractive axisymmetric design should be

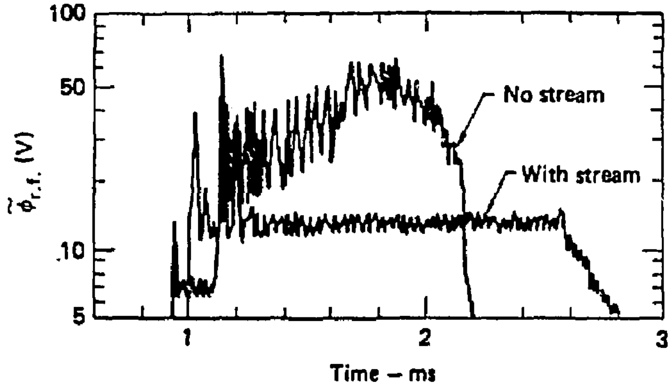

Figure 2: Experimental observation of rf fluctuations in 2XIIB.

possible with the 8 T version, obtaining MHD stability from the warm plasma pressure in good-curvature regions outside the mirrors, as in the Gas Dynamic Trap [5].

3. Microstability

3.1. Drift-Cyclotron-Loss-Cone Mode

The 2XIIB experiments reduced microinstabilities to a residual level that did not significantly reduce the energy or particle confinement time of energetic neutral-beam-injected ions. This stabilization was accomplished by use of a warm streaming plasma, provided either with stream guns [6] or a gas box [7]. The term "stream" refers to an unconfined plasma. Figure 2 shows the effect of the stream in reducing the floating potential fluctuation level.

As a result of reduced microinstability levels, the hot-ion cooling rate became classical and was dominated by electron drag in the high stream current limit appropriate to a neutron source. This result is shown in Fig. 3 [8].

The residual-level instability was identified as the drift-cyclotron-loss-cone DCLC mode based on the frequency, which was in a narrow band ($\Delta f/f < 0.02$) near the ion-cyclotron frequency (corrected for finite beta) and the second harmonic, and on the perpendicular

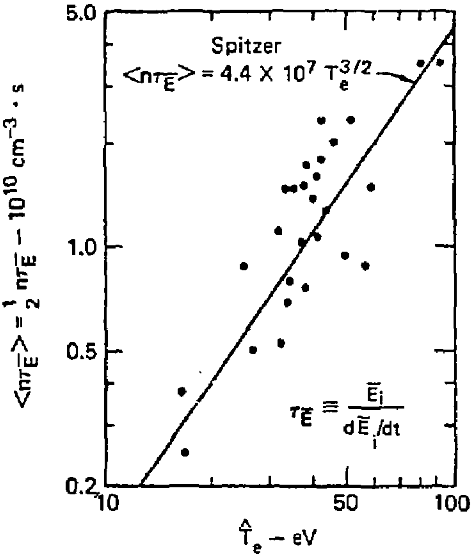

Figure 3: The ion energy confinement time in 2XIIB is dominated by electron drag.

wave number $k_\perp = 0.51 \pm 0.10$ cm^{-1} propagating in the ion-diamagnetic direction. Theory predicts the instability at the cyclotron frequency with $k_\perp \approx 0.7$ cm^{-1}, in agreement with the experiment [9]. The first identification of the DCLC mode was made in the PR-6 experiment [10] and subsequently in the 2XII experiment [11].

The stream plasma was injected as cold plasma ($\leq$ 10 eV) from a plasma gun at the end wall, or from a gas box near the mirror in 2XIIB. Good agreement with experimental confinement time and warm plasma fraction was obtained by the Baldwin-Berk-Pearlstein (BBP) model [12] that computes the marginally stable level of DCLC oscillations required to heat the cold plasma to fill the ambipolar hole in velocity space sufficiently to maintain the fluctuation level. Measurements of the rate at which ions diffuse to higher energy during plasma decay, after the stabilizing plasma stream was turned off, agreed with computed DCLC diffusion rates (see Fig. 4) [13]. While the plasma stream was on, the fluctuation level was too low (see Fig. 2), for significant energy diffusion to occur.

An alternative interpretation of the data was proposed by Clauser [14]. He suggested that

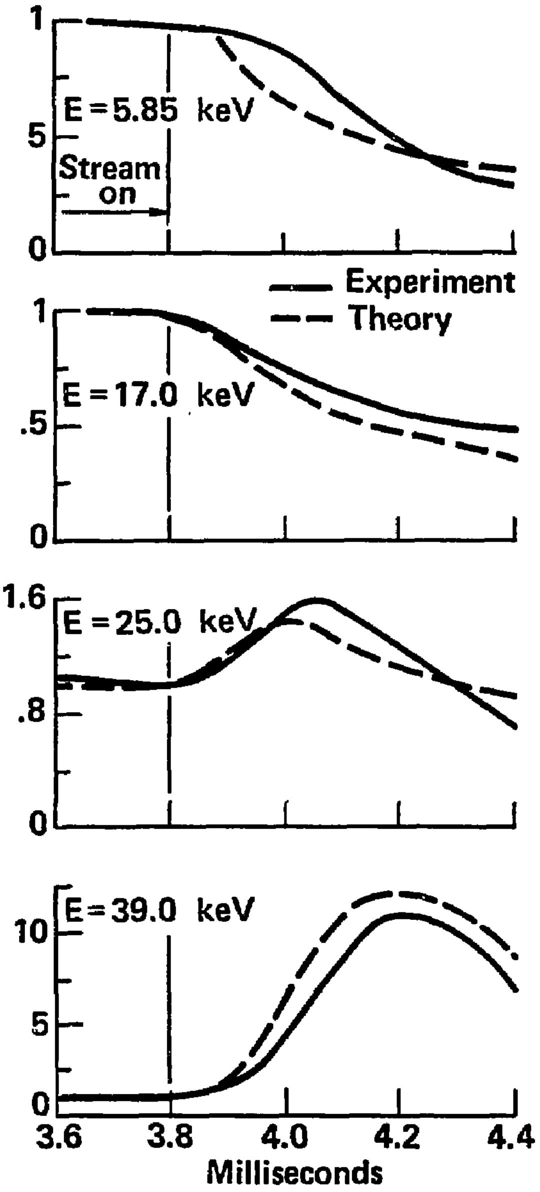

Figure 4: Experimental and theoretical time behavior of ion energy-distribution function of 5.9, 17, 25, and 39 keV. The theoretical quasilinear diffusion curves are normalized to experimental data at 3.8 ms.

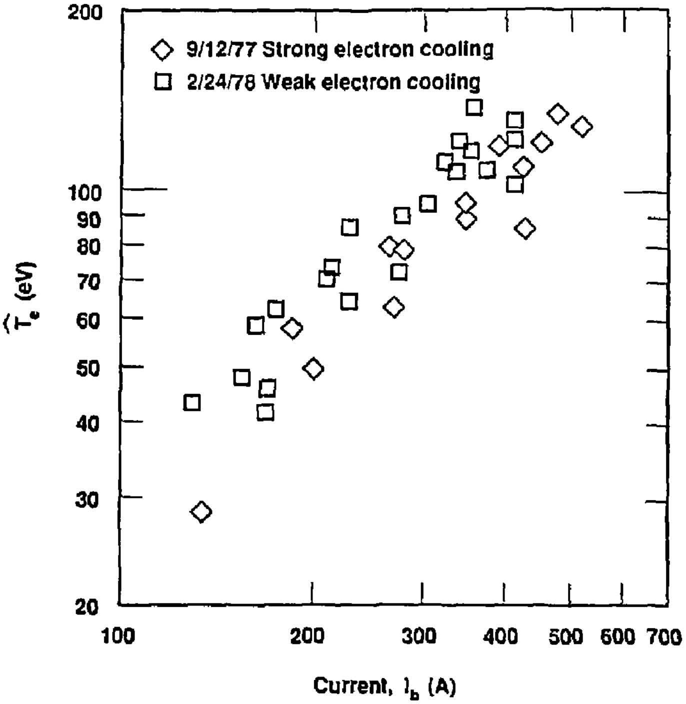

Figure 5: The linear dependence of $\hat{T}_e$ on neutral-beam current is consistent with the latter supplying sufficient warm ions for microstability.

the only effect of the warm plasma was to reduce the electron temperature, and therefore the ambipolar hole, such that the neutral-beam-injected current (as it lost energy due to electron drag or quasilinear diffusion) was sufficient to *fill* the hole, producing marginal stability. This interpretation is consistent with the linear dependence of electron temperature T_e on neutral-beam current (see Fig. 5); because higher beam current provided more stream current to fill a larger ambipolar hole. Clauser also found that the theoretically required stream current showed little correlation with the total stream current (injected gas plus trapped beam current—see Fig. 6a), but correlated well with the trapped beam current (see Fig. 6b).

Additional evidence for and against Clauser's interpretation comes from experiments shown in Fig. 7 using neon-fed arc plasma guns at the end wall. These experiments showed

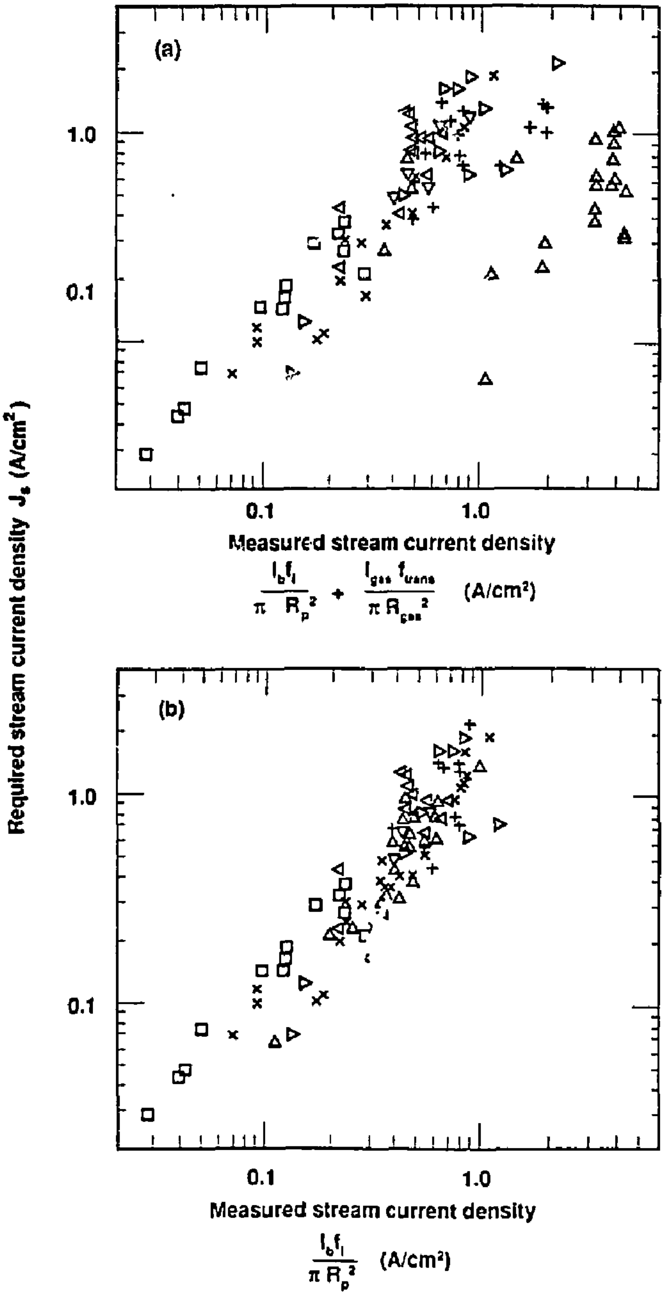

Figure 6: The theoretically required stream current on axis for microstability (a) does not correlate well with the total measured stream (gas plus beams), but (b) does correlate well with the neutral beam current alone.

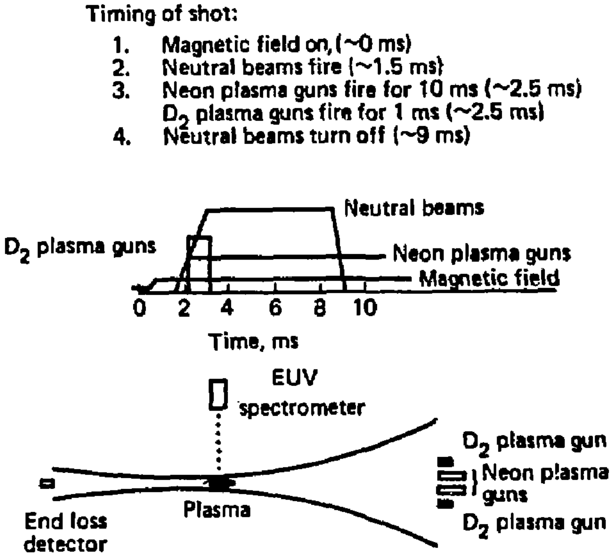

Timing of shot:
1. Magnetic field on, (~0 ms)
2. Neutral beams fire (~1.5 ms)
3. Neon plasma guns fire for 10 ms (~2.5 ms)
   D_2 plasma guns fire for 1 ms (~2.5 ms)
4. Neutral beams turn off (~9 ms)

Figure 7: Schematic of the neon-plasma-injection experiment.

that plasma could be sustained using only the neon-fed guns, with plasma parameters similar to those obtained with the standard deuterium-fed guns (see Table 3 and Ref. 15). This evidence implies that the plasma was reasonably microstable because it could not be sustained without some warm plasma source. The data are consistent with Clauser's model that the electron temperature adjusts until ionization of the neutral beam is sufficient to fill the ambipolar hole, when the beam ions drag or scatter down in energy [14]. For the data in Table 3, the ionized beam current (on only the hot ions) is 31-A, which is comparable to the 39-A value measured with an end-loss-analyzer across the 12.5 cm radius plasma.

On the other hand, the microinstability level is higher with a neon stream. Figure 8 shows that both the microwave scattering and the 25-keV charge-exchange signal are higher by a factor of 2 to 3 with neon than with deuterium stream guns. The 25 keV ions are a result of up-scattering of the 18 to 20 keV neutral-beam-injected ions. This results in a

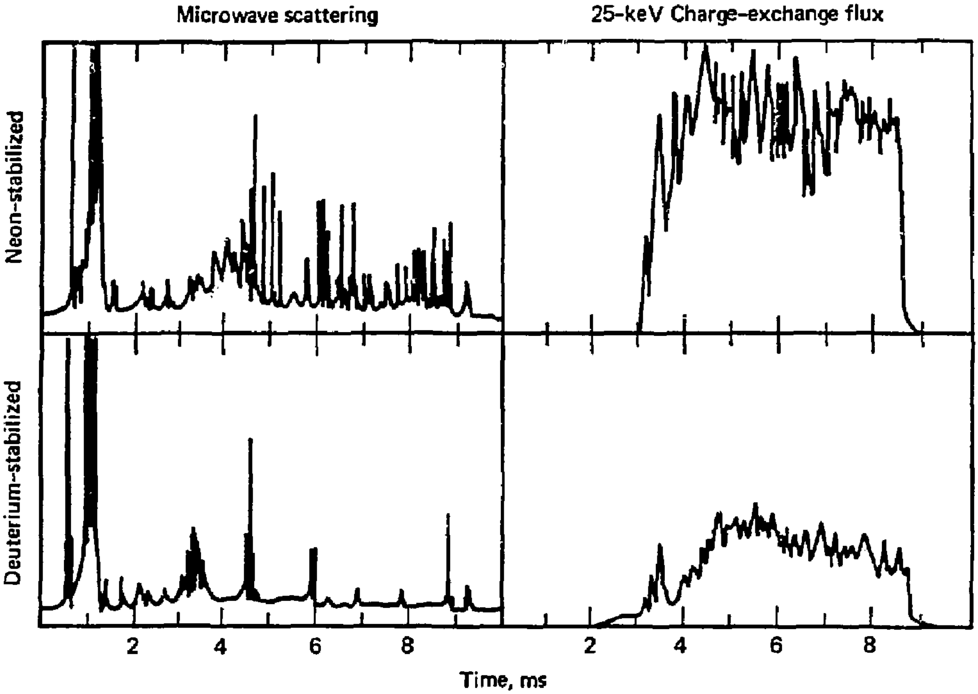

Figure 8: Either neon or deuterium gas stabilizes the plasma. More intense fluctuations are observed with neon.

slightly higher ion energy of 12 keV with neon, versus 10 keV with deuterium stream guns (see Table 3). Such results indicate that a neon stream is less effective than a deuterium stream in stabilizing. We conclude that Clauser's model predicts the macroscopic plasma parameters quite well; it fails only to predict the microinstability levels with nonhydrogenic plasma stream.

We have evaluated a 4 T, 50 MW neutron source design [1] for stability to DCLC using Clauser's model, which requires lower electron temperatures than does the BBP model [12]. We found that his criterion would allow electron temperatures up to 450 eV for marginal DCLC stability [16]. Such temperatures are more than double the 190 eV resulting from Spitzer conductivity, which determines T_e from the axial power balance. Therefore, we expect

Table 3: Plasma parameters during plasma injection.

Parameter	Symbol	Neon-stabilized	Deuterium-stabilized
Line density	$\int n_e dl$	5.5×10^{14} cm^{-2}	
Density	n		5.0×10^{14} cm^{-3}
Plasma radius	R_p	12.5 cm	11 cm
Peak density	$\hat{n}_e$	2.6×10^{13} cm^{-3}	2.6×10^{13} cm^{-3}
Electron temperature	T_e	50 eV	50 eV
West end loss at midplane	j	40 mA/cm^2	100 mA/cm^2
Neutral-beam current	I_b	390 A	390 A
Plasma diamagnetism	$\nabla\phi$	720 A · m^2	720 A · m^2
Mean ion energy	W	12 keV	10 keV
Neon density	N	6.8×10^{10} cm^{-3}	

a neutron source to be DCLC stable because it satisfies the most restrictive microstability criterion with a significant safety margin.

In addition, we expect that the residual DCLC instability level will be much lower in a neutron source than in 2XIIB. First, in terms of the BBP model, cold ions originating from recycling near the end wall of a beam-plasma neutron source undergo many collisions before diffusing to the neutron cell. These collisions heat them to the order of $T_i \approx T_e$, greatly reducing the instability level required to heat the warm ions. It may even eliminate the need for marginal stability level oscillations. Second, in terms of Clauser's model, T_e is less than one-half the value that would provide marginal stability, so that electron drag is both increased and has a smaller ambipolar hole to fill. We therefore expect electron drag to be sufficient to fill the ambipolar hole without the aid of DCLC fluctuations.

3.2. *Alfven-Ion-Cyclotron Mode*

The Alfven-ion-cyclotron (AIC) mode was identified on TMX [17], but was not identified on 2XIIB. This result is not unexpected because the 2XIIB plasma had a smaller product of βA^2, where $A =< W_\perp > / < W_\parallel >$ is the anisotropy, which was twice as large in TMX as in 2XIIB. Furthermore, less anisotropy is required to drive the AIC unstable when r_p/a_i increases, as it did in TMX [17]. In TMX, the AIC generally propagated in the

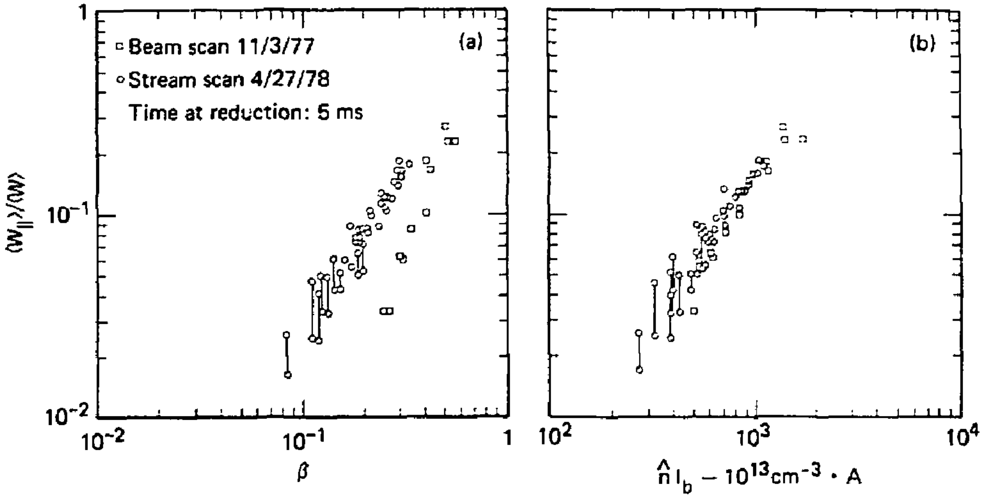

Figure 9: Angular spread of ions in 2XIIB vs (a) β at plasma center and (b) the product of peak ion density and neutral-beam current $\hat{n}I_b$. Vertical lines indicate the range during bursting.

electron diamagnetic direction, with a frequency of about 0.9 of the beta-depressed cyclotron frequency, and azimuthal mode numbers of 2 to 4 [17].

The AIC may have been stabilized in 2XIIB by the spreading of the hot-ion angular-distribution in the deeper well dug by the beta of the plasma. This spreading was measured by Nexsen [19] from the reduction in perpendicular charge-exchange flux relative to the product of plasma density times beam current, Fig. 9. However, instabilities in 2XIIB were observed to propagate in the opposite direction as the ion diamagnetic drift very early or late in time [9]. Casper notes that these instabilities may well have been AIC [18].

The neutron source is not so obviously stable to the AIC as to the DCLC instability We believe that the stabilizing factors, especially the high density of warm plasma as well as the moderate beta of only 20% in the recent 8-T design, will more than counteract the larger radius and large anisotropy (comparable to 2XIIB or TMX) in the neutron source. We expect greater stability to the AIC mode in the neutron source than in either 2XIIB or TMX.

4. Plasma Startup

The 2XIIB experiments demonstrated the startup of a neutral beam-sustained plasma by injecting beams into the warm plasma formed with a stream gun at an end wall [20]. Within 2 ms, the plasma density exponentiated to 4×10^{13} cm^{-3}, and beta reached 0.4, driven by the injection of 310 A equivalent of 14 keV neutral beams. Even higher parameters, densities reaching 10^{14} cm^{-3} and betas greater than unity, were achieved by switching the source of the stabilizing stream plasma to a gas box after the initial plasma formation [7]. (Continuation of this work led to peak beta near 2 [3]). All of these cases were fit by a simple time-dependent buildup model that balanced beam trapping against losses due to a fixed confinement $n\tau$ (see Fig. 10). Here,

$$\frac{dn_t}{dt} = \frac{(<\sigma_i v> + <\sigma_x v>) l_s f_s n_s}{v_b e V_t} + \frac{<\sigma_i v> l_t f_t I n_t}{v_b e V_t} - \frac{n_t}{\tau}, \tag{1}$$

where $\sigma_{i,x}$ are the ionization and charge-exchange cross-sections, and v_b and v are the neutral-beam and relative particle-beam velocities averaged over the measured ion distribution. The beam trapping efficiency f is averaged over the profiles of plasma density n and beam current I. The plasma volume is V, the diameter is l, and the lifetime is τ. The subscripts s and t refer to streaming and trapped plasma, respectively.

Startup with a single, circular plasma gun on the axis yielded an elliptical plasma at the midplane of the minimum-B mirror cell. Within 1 m, this plasma became circular [20]. However, greater assurance of producing a plasma of larger radius was provided by using multiple stream guns from both ends that provided a stream plasma mapping at the midplane, as shown in Fig. 11. With this arrangement, plasma of radius up to $r_p/ai = 6$ were achieved [4]. Attempts to produce larger plasmas resulted in hollow density profiles. However, up to $r_p/ai = 6$, the plasma profile was Gaussian as shown in Fig. 12.

Having demonstrated that the startup model fit 2XIIB, we can now apply it to the neutron source with two modifications. First, we replace the fixed-loss time $n\tau$ with the time for electron drag to drag ions from the injection energy down to the energy of the ambipolar

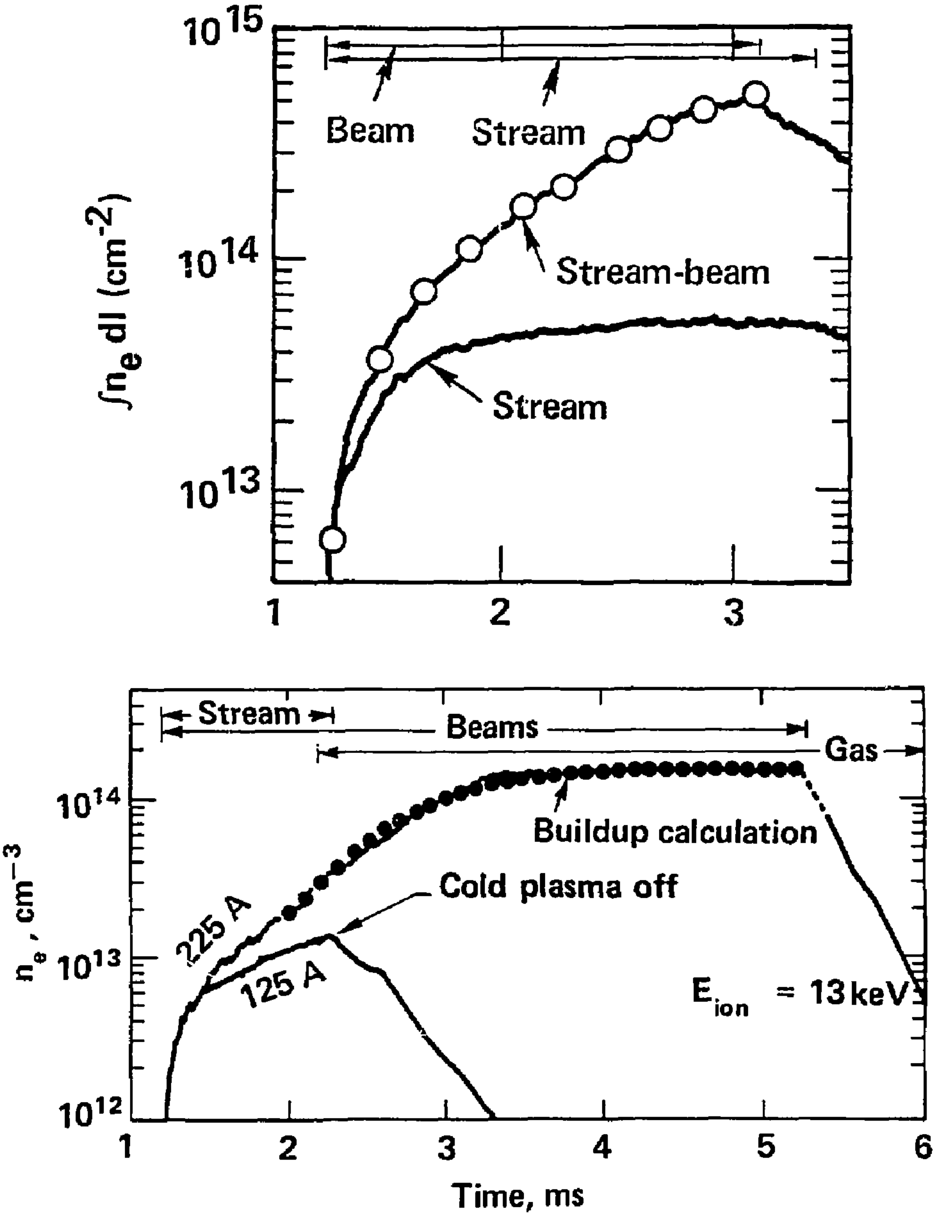

Figure 10: Density buildup history on streaming plasma target showing (a) $\int n_e d\ell$ with stream guns and (b) $\bar{n}_e$ with 8000-A hydrogen gas feed. The circular points are computed with the buildup model.

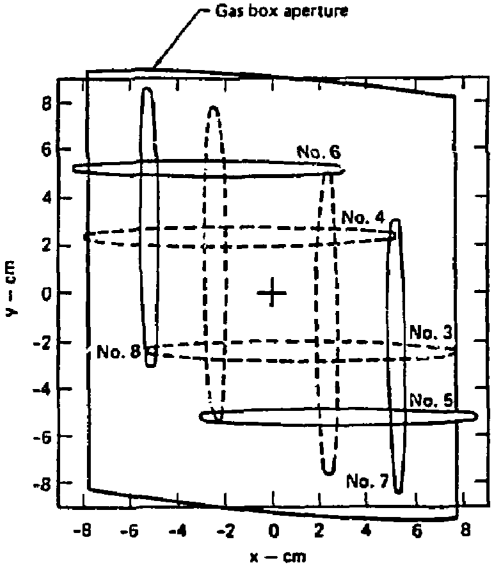

Figure 11: Vacuum magnetic-field mappings of streaming-gun plasma and gas-box aperture at the midplane for $B_{vac} = 0.67$ T, including a 0.2-T dc guide field.

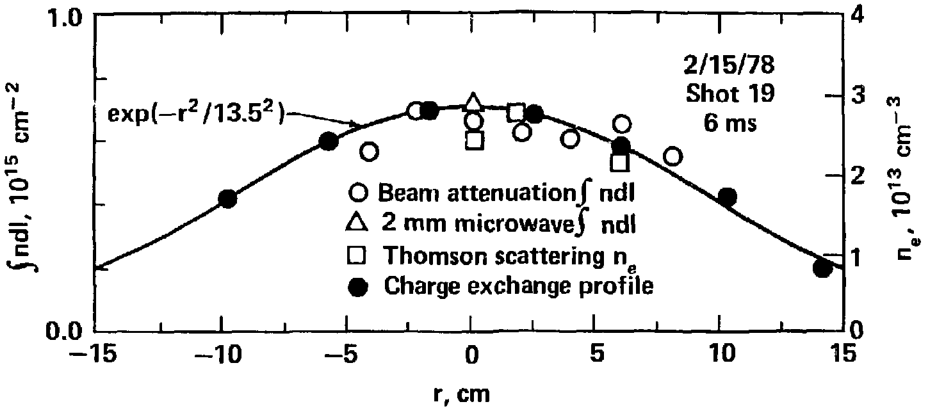

Gaussian radius

Charge exchange scan $R_p = 13.5$ cm

Beam attenuation $R_p = 13.0$ cm

Microwave $\int ndl/\sqrt{\pi}$ laser n_e $R_p = 14.4$ cm

Vacuum gyro radius

Hydrogen

$\bar{W}_i = 10$ keV

B = 0.77 T

$a_i = 1.9$ cm

$R_p/a_i = 7.2$

Figure 12: Radial density profiles of large-diameter 2XIIB plasma.

hole (5 to 7 times the drag time). Second, as discussed under DCLC microstability, T_e is lower with Spitzer conduction to the ends than would be required for DCLC stability. However, the plasma is not dominated by Spitzer conduction until the plasma column has built up to a sufficient density. Therefore, the second modification is to assume flow-dominated losses and to adjust the stream current to high enough values to produce the same steady state $T_e = 190$ eV that is produced by Spitzer conduction. We compute the buildup to steady-state to occur in a few milliseconds [16]. Figure 13(a) through (c) shows these results in terms of the buildup of density, electron temperature, and gas input current. The latter value reaches 30,000 A, which is twice the gas current injected into 2XIIB, as discussed in Section 6.

5. Cold Ions Fuel Midplane

The 2XIIB experiments demonstrated that ions injected from the gas box near a mirror would penetrate through the plasma to the midplane and the far end, if the gas current were sufficiently great (see Fig. 14) [14]. For lower gas currents, all the cold ions were measured to come out at the gas box end; whereas, above the critical current, only about one-half of the ions came out that end. The remainder apparently reached the midplane, and then were lost to the other end. This result is consistent with a simple model, where the density and potential at the gas box increase with gas current. When the gas box potential is less than the midplane potential, all ions are reflected. When the gas box potential exceeds the midplane potential, half of the cold ions are transmitted. Consideration of either this or a simple axial-density diffusion model implies that the midplane of a beam-plasma neutron source can be fueled by warm ions by using sufficient gas at the end walls. This enables operation in a two-component mode where most collisions of energetic deuterium ions are with warm tritium ions.

Hot Ion &Total Density Buildup VS Time (0.1 msec)

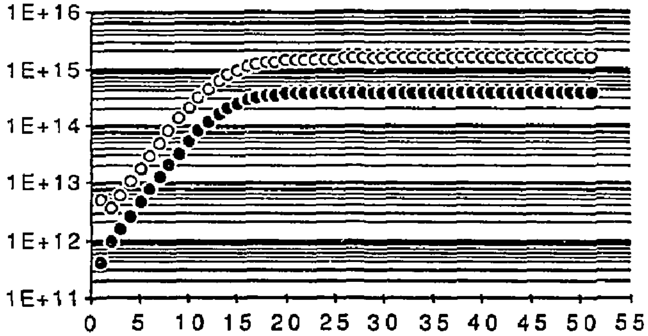

Electron Temperature VS Time (0.1 msec)

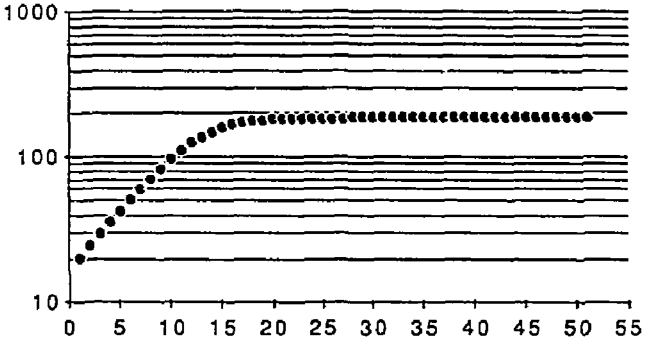

Gas Input Current (Amps) VS Time (0.1 msec)

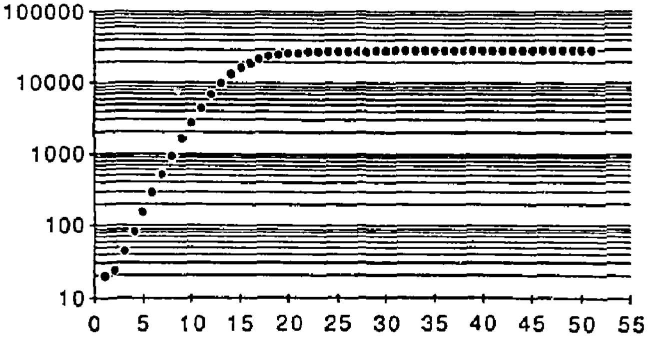

Figure 13: The startup of a 4-T beam-plasma neutron source is computed with the buildup model showing (a) hot-ion and total density buildup, (b) electron temperature, and (c) gas input current over time.

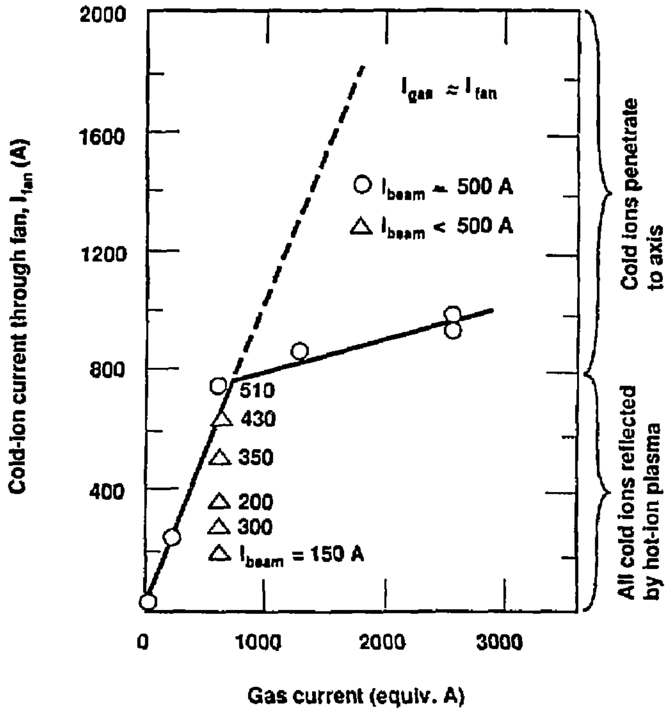

Figure 14: Cold-ion current through the west fan at constant neutral-beam current $I_b \approx$ 500 A is equal to the gas-fed current up to $\sim I_{gas} = 650$ A; because cold ions from the gas box are reflected by the central plasma. Above 650 A, cold ions start penetrating the central barrier, as is evidenced by change in slope.

6. Variation of T_e Along a Field Line

Substantial gradients in T_e along the magnetic field were observed in 2XIIB. Figure 15 shows measurements of T_e versus axial position [14], where $T_e(z)$ is seen to vary by factors of 3 to 10. The variation in T_e increases with the gas-feed current or pressure. Similar gradients in T_e are required in a neutron source to remove the trapped neutral-beam power along the axis by thermal conduction. We conclude that the observed gradients of T_e in 2XIIB were similar to those required in a neutron source and the maximum gas-feed current of 15,600 A was within a factor of two at the gas-feed current required during start-up of a beam-plasma neutron source.

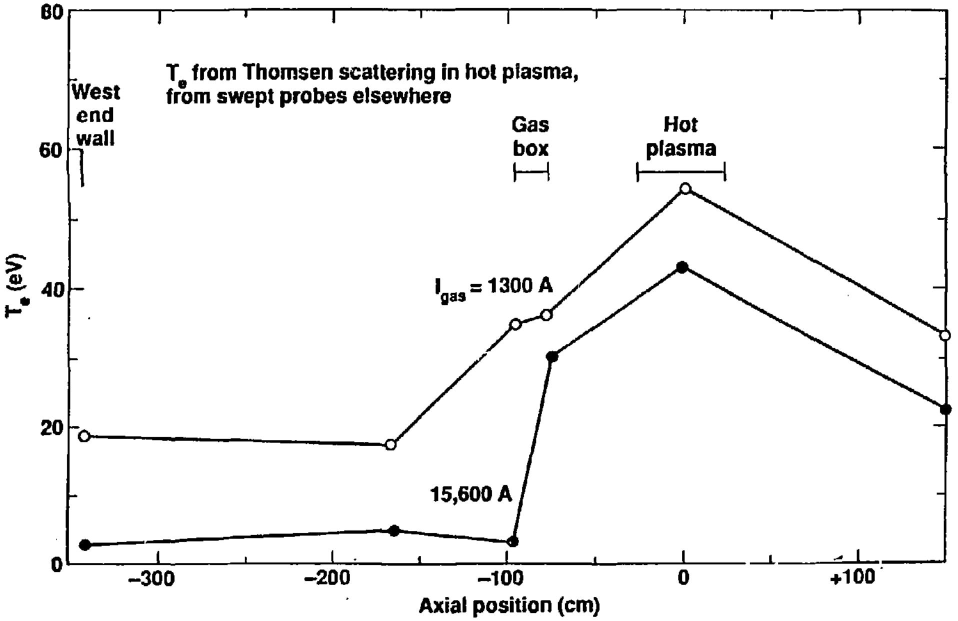

Figure 15: Axial gradients of electron temperature near the gas feed location are observed with high gas-feed rates in 2XIIB.

References

[1] F.H. Coensgen, T.A. Casper, D.L. Correll, C.C. Damm, A.H. Futch, B.G. Logan, A.W. Molvik, and R.H. Bulmer, Lawrence Livermore National Laboratory, UCRL-97280 (1987).

[2] F.H. Coensgen, et al., in preparation.

[3] W.C. Turner, et al., *Nucl. Fusion* **19**, 1011 (1979).

[4] D.L. Correll, et al., *Nucl. Fusion* **20**, 655 (1980).

[5] A. Bagryanskii, G.V. Roslyakov, et al., IAEA Kyoto, 1986; T.A. Casper, A.W. Molvik, P.A. Bagryanskii, et al., post-deadline paper, *Bull. Am. Phys. Soc.* **33**, (Oct. 1988).

[6] F.H. Coensgen, et al., *Phys. Rev. Lett.* **35**, 1501 (1975).

[7] B.G. Logan, et al., *Phys. Rev. Lett.* **37**, 1468 (1976).

[8] F.H. Coensgen and T.C. Simonen, Varenna (1979).

[9] W.C. Turner, E.J. Powers, and T.C. Simonen, *Phys. Rev. Lett.* **39**, 1087 (1977).

[10] M.S. Ioffe, B.I. Kanaev, V.P. Pastukhov, and E.E. Yushmanav, *Sov. Phys. JETP* **40**, 1064 (1975).

[11] T.C. Simonen, *Phys. Fluids* **19**, 1365 (1976).

[12] D.E. Baldwin, H.L. Berk, and L.D. Pealstein, *Phys. Rev. Lett.* **36**, 1051 (1976).

[13] W.C. Turner, H.L. Berk, and J.J. Stewart, Lawrence Livermore National Laboratory, UCRL-78673 (1976).

[14] J. Clauser, unpublished LLNL report partially published in *Magnetic Fusion Energy Annual Report, Oct 76-Sept. 77*, Lawrence Livermore National Laboratory, UCRL-50002-

77 (1978); B.I. Cohen, et al., Lawrence Livermore National Laboratory, UCRL-83517 (1980).

[15] R.P. Drake, Lawrence Livermore National Laboratory, UCRL-52751 (1980), section VI, and appendix G2.

[16] A.W. Molvik, "Startup and Shutdown of an Intense Neutron Source," Lawrence Livermore National Laboratory, memorandum, Feb. 11, 1988.

[17] T.A. Casper and Gary R. Smith, *Phys. Rev. Lett.* **48**, 1015 (1982).

[18] T.A. Casper, Lawrence Livermore National Laboratory, private communication.

[19] W.E. Nexsen, Jr., in *Magnetic Fusion Energy Quarterly Report, Oct.-Dec. 1978,* Lawrence Livermore National Laboratory, UCRL-50051-78-4 (1979).

[20] F.H. Coensgen, et al., *Phys. Rev. Lett.* **37**, 143 (1976).